Coexistence of spontaneous dimerization and magnetic order in a transverse-field Ising ladder with four-spin interactions

J. C. Xavier [,1] R. G. Pereira [,2] M. E. S. Nunes [,3] and J. A. Plascak [4,5,6]

[1]*Universidade Federal de Uberlândia, Instituto de Física, C. P 593, 38400-902 Uberlândia, MG, Brazil*
[2]*International Institute of Physics and Departamento de Física Teórica e Experimental,*
Universidade Federal do Rio Grande do Norte, 59072-970 Natal, RN, Brazil
[3]*Universidade Federal de Ouro Preto, Departamento de Física, ICEB, Campus Universitário Morro do Cruzeiro,*
35400-000 Ouro Preto, MG, Brazil
[4]*Universidade Federal da Paraíba, Departamento de Física, CCEN, Campus I, s/n, Cidade Universitária,*
58051-090 João Pessoa, PB, Brazil
[5]*Departamento de Física, Instituto de Ciências Exatas, Universidade Federal de Minas Gerais, C.P. 702,*
30123-970 Belo Horizonte, MG, Brazil
[6]*Department of Physics and Astronomy, University of Georgia, Athens, Georgia 30602, USA*

The spin-1/2 transverse field two-leg Ising ladder with nearest-neighbor exchange and plaquette four-spin interaction J_4 is studied analytically and numerically with the density matrix renormalization group approach. The quantum phase diagram in the transverse field B versus J_4 plane has been obtained. There are three different phases: a paramagnetic (PM) phase for high values of the transverse field and, for low values of B, a ferromagnetic (FM) ordered phase for small J_4, and a dimerized-rung (DR) phase for large negative values of J_4. All phases are separated by quantum phase transition lines meeting at a multicritical point. The critical lines have been obtained by exploring the entanglement entropy. The results show that along the critical lines the central charge is $c = 1/2$, while at the multicritical point one has $c = 1$. The scaling dimension of the energy operator is $X_\epsilon = 1$, in agreement with the universality class of the critical behavior of the quantum Ising chain. An effective field theory for the multicritical point is also discussed. The FM and the DR order parameters have also been computed and we found a region where the FM and the DR phases coexist.

I. INTRODUCTION

The topic of quantum spin systems is by far one of the most fascinating and interesting branches of experimental and theoretical physics. Although in the beginning the study of quantum spin systems was specifically related to magnetism and the corresponding magnetic properties [1,2], it has by now migrated to several areas such as high-temperature superconductors [3], ferromagnetic nanowires [4], and spintronics [5], among others. Quantum phase transitions have also been recently revisited and a close analogy to the simple fluid phase diagram has been experimentally detected in the geometrically frustrated quantum antiferromagnet $SrCu_2(BO_3)_2$ [6].

Low-dimensional quantum spin models with competing interactions represent a fertile ground for unconventional magnetic behavior. Examples in one dimension include the transverse Ising model with next-nearest-neighbor interactions [7] and with linear interaction among four spins [8–10], ladder models describing cuprates [11,12], and spin models with four-spin interactions used to explain ferroelectrics [13–15]. Zero-dimensional models are also important when applied to magnetic molecules and nanomagnetism [16–18], multiferroics [19,20], and ultracold atoms trapped in optical lattices [21,22].

While nearest-neighbor exchange is often the dominant interaction in Mott insulating materials, longer-range and multispin interactions may play an important role, particularly in the vicinity of a metal-insulator transition [23,24]. In fact, the ring exchange interaction has been invoked to reproduce the dispersion relation observed in inelastic neutron scattering experiments on cuprates such as La_2CuO_4 and $La_6Ca_8Cu_24O_41$ [25–28]. More recently, four-spin interactions have been argued to stabilize a chiral spin liquid on the triangular lattice [29].

Motivated by experiments on materials with a ladderlike structure [30–34], spin ladder models have been extensively studied and shown to display rich phase diagrams. For instance, the frustrated antiferromagnetic spin ladder in a magnetic field exhibits a magnetization plateau at half saturation which is attributed to a gapped state that spontaneously breaks the lattice translational symmetry [35–37]. A columnar dimer phase was also proposed at zero magnetic field [38,39], but the numerical evidence for this phase is still ambiguous [40]. Moreover, four-spin interactions in spin ladders can give rise to other unusual types of order, such as scalar chirality and intraleg staggered dimerization [41–46].

The purpose of the present work is to study the effects of four-spin interactions on the transverse-field Ising model

defined on a two-leg ladder. Based on analytical consider-
ations and density matrix renormalization group (DMRG)
methods, we map out the phase diagram of the model and
characterize the nature of the transitions. In the regime of
dominant four-spin interaction, we find a nonmagnetic phase
which breaks translational invariance by means of rung dimer-
ization. Remarkably, for intermediate values of the four-spin
interaction this dimer order coexists with the conventional
ferromagnetic (FM) order of the quantum Ising model at weak
fields. Analyzing the entanglement entropy, we identify two
critical lines in the Ising universality class, with central charge
$c = 1/2$. These lines cross at a multicritical point with central
charge $c = 1$, below which the coexistence phase appears.

The paper is organized as follows. In Sec. II we introduce
the model and discuss the phases for some simple limits of
the parameters. The determination of the critical behavior,
using the entanglement entropy and the DMRG procedure,
is described in Sec. III. Our main results are presented in
Sec. IV. Finally, some concluding remarks are left for Sec. V.

II. MODEL AND PHASES

Consider the following Hamiltonian for a two-leg quantum
Ising ladder with periodic boundary conditions (PBC):

$$\mathcal{H} = -\sum_{n=1,2}\sum_{i=1}^{L}\left(\sigma_{n,i}^{z}\sigma_{n,i+1}^{z} + B\sigma_{n,i}^{x}\right)$$
$$-\sum_{i=1}^{L}\left(J_{\perp}^{z}\sigma_{1,i}^{z}\sigma_{2,i}^{z} + J_{4}\sigma_{1,i}^{z}\sigma_{1,i+1}^{z}\sigma_{2,i}^{z}\sigma_{2,i+1}^{z}\right). \quad (1)$$

Here $\sigma_{n,i}^{\eta}$ ($\eta = x, z, y$) are the Pauli spin matrices at the ith site
of leg $n = 1, 2$ and L is the length of the ladder, which has a
total of $N = 2L$ sites. The first term with a coupling constant
set to unity corresponds to the Ising interaction along the legs.
In addition to a transverse magnetic field B, the Hamilto-
nian includes a rung coupling $J_{\perp}^{z}$ in the z spin direction as
well as a four-spin interaction J_{4} on square plaquettes. For
$J_{\perp}^{z} = J_{4} = 0$, the model reduces to two decoupled transverse-
field Ising chains. For $J_{\perp}^{z} = 0$ but $J_{4} \neq 0$, the model has a
$\mathbb{Z}_{2} \times \mathbb{Z}_{2}$ symmetry in analogy with the quantum Ashkin-
Teller model [47,48]. This $\mathbb{Z}_{2} \times \mathbb{Z}_{2}$ symmetry is generated
by $\mathcal{R}_{n} = \prod_{i}\sigma_{n,i}^{x}$ with $n = 1, 2$ and is equivalent to global
π rotations around the x axis for each leg independently. In
the complete model, the $J_{\perp}^{z}$ interaction breaks this symmetry
down to a single $\mathbb{Z}_{2}$ symmetry generated by $\mathcal{R} = \mathcal{R}_{1}\mathcal{R}_{2}$.
Hereafter we set $J_{\perp}^{z} = 1$, which describes a spatially isotropic
transverse-field Ising ladder supplemented by four-spin
interactions.

We are interested in the ground state (GS) phase diagram of
the model as a function of $B > 0$ and $J_{4} < 0$. To gain insight
into the possible phases, let us consider some particular limits
of the Hamiltonian parameters. For $J_{4} = 0$, the physics is
governed by the competition between the ferromagnetic Ising
coupling and the transverse magnetic field. In this limit we
expect a continuous phase transition in the two-dimensional
Ising universality class from a FM phase for $B < B_{c}$ to a
paramagnetic (PM) phase for $B > B_{c}$. The FM phase has two
degenerate ground states that spontaneously break the $\mathcal{R}$ sym-
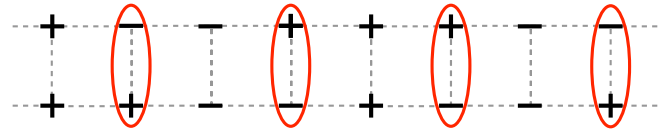metry. In a four-site plaquette, the classical FM ground states

FIG. 1. Sketch of the dimerized-rung phase. The enclosed up-
down dimers are located in one sublattice.

can be represented by $\begin{smallmatrix}+\\+\end{smallmatrix}$ $\begin{smallmatrix}+\\+\end{smallmatrix}$ and $\begin{smallmatrix}-\\-\end{smallmatrix}$ $\begin{smallmatrix}-\\-\end{smallmatrix}$, where $\pm$ denotes
a spin polarized in the $\pm\hat{z}$ direction. In the PM phase, the
unique GS is adiabatically connected with the product state
with all spins polarized in the $\hat{x}$ direction. On the other hand,
for $B = 0$ and $J_{4} \neq 0$ we have a classical Ising model with
four-spin interactions. While $J_{4} > 0$ favors the FM states, for
$J_{4} < -3/2$ we find a new type of order that we refer to as
the dimerized-rung (DR) phase, which we will discuss in the
following.

The classical GSs of the DR phase obey the local constraint
that all plaquettes have only one spin with a different sign.
An example is sketched in Fig. 1. Importantly, the constraint
implies an alternation between rungs with parallel or antipar-
allel spins. Here it is convenient to introduce the pseudospins
$T_{i}^{z} = \sigma_{1,i}^{z}\sigma_{2,i}^{z}$ and $S_{i}^{z} = \sigma_{1,i}^{z}$ and represent states in the local
basis for each rung by $|T_{i}^{z}, S_{i}^{z}\rangle$. The subspace of classical DR
states with energy $E_{0} = -L|J_{4}|$ is then defined by $T_{i+1}^{z} = -T_{i}^{z}$
with arbitrary $\{S_{i}^{z}\}$. As a consequence, the DR states break
translational symmetry $i \mapsto i + 1$ upon the choice of antipar-
allel spins $T^{z} = -$ on the even or odd sublattice. We refer
to a rung with antiparallel spins as an up-down dimer. The
classical GS degeneracy is given by 2^{L+1}. We stress that the
DR phase should not be confused with the rung singlet phase
that appears in the case of isotropic spin interaction [42].
Unlike the DR phase, the rung singlet phase does not break
any symmetries and has a unique ground state.

A small transverse magnetic field must lift the exponential
degeneracy of the classical model. To see this effect, we first
rewrite the Hamiltonian in terms of the rung pseudospins:

$$\mathcal{H} = -\sum_{i=1}^{L}\left[J_{4}T_{i}^{z}T_{i+1}^{z} + \left(1 + T_{i}^{z}T_{i+1}^{z}\right)S_{i}^{z}S_{i+1}^{z} + T_{i}^{z}\right]$$
$$-B\sum_{i=1}^{L}\left(1 + S_{i}^{x}\right)T_{i}^{x}, \quad (2)$$

where $T_{i}^{x} = \sigma_{2,i}^{x}$ and $S_{i}^{x} = \sigma_{1,i}^{x}\sigma_{2,i}^{x}$, so that the pseudospins
obey $\{T_{i}^{x}, T_{i}^{z}\} = \{S_{i}^{x}, S_{i}^{z}\} = 0$ and $[T_{i}^{x}, S_{i}^{z}] = [S_{i}^{x}, T_{i}^{z}] = 0$. In
this notation, the global π rotation is written as $\mathcal{R} = \prod_{i}S_{i}^{x}$.
The analysis of the Hamiltonian becomes particularly simple
in the limit $|J_{4}|, B \gg 1$. Dropping the exchange interaction
terms, we obtain

$$\mathcal{H} \approx -\sum_{i=1}^{L}\left[J_{4}T_{i}^{z}T_{i+1}^{z} + B\left(1 + S_{i}^{x}\right)T_{i}^{x}\right]. \quad (3)$$

In this limit, the operators S_{i}^{x} become conserved quantities. If
we fix $S_{i}^{x} = +1$ for all rungs, the model reduces to an Ising
chain with a uniform transverse field for the T pseudospins.

In terms of the original spins, the state on each rung becomes a superposition:

$$|T^z = +, S^x = +\rangle = \frac{1}{\sqrt{2}}\left(\left|\begin{matrix}+\\+\end{matrix}\right\rangle + \left|\begin{matrix}-\\-\end{matrix}\right\rangle\right), \qquad (4)$$

$$|T^z = -, S^x = +\rangle = \frac{1}{\sqrt{2}}\left(\left|\begin{matrix}+\\-\end{matrix}\right\rangle + \left|\begin{matrix}-\\+\end{matrix}\right\rangle\right). \qquad (5)$$

From now on we are going to consider only negative values of J_4. For $B \ll -J_4$, the GSs are selected within the sector with $T^z_{i+1} = -T^z_i$. The only remaining degeneracy is that associated with the broken translational invariance. The two GSs can be viewed as crystals of up-down dimers and are distinguished by the order parameter

$$D = \frac{1}{L}\sum_{i=1}^{L}(-1)^i\langle T^z_i\rangle = \frac{1}{L}\sum_{i=1}^{L}(-1)^i\langle\sigma^z_{1,i}\sigma^z_{2,i}\rangle. \qquad (6)$$

Remarkably, the excited states with energy $\sim B \ll |J_4|$ also originate from the sector with the local constraint $T^z_{i+1} = -T^z_i$; thus, they all have $D \neq 0$ in the thermodynamic limit. The elementary excitation in the regime $B \ll |J_4|$ corresponds to inverting the eigenvalue of S^x_i, by applying a phase flip to the rung state

$$\left|\begin{matrix}\sigma^z_1\\\sigma^z_2\end{matrix}\right\rangle \mapsto \sigma^z_1\left|\begin{matrix}\sigma^z_1\\\sigma^z_2\end{matrix}\right\rangle, \qquad (7)$$

without disrupting the long-range DR order.

As we increase the magnetic field in the regime $B, |J_4| \gg 1$, the quantum fluctuations suppress the DR order. According to Hamiltonian (3), there is an Ising transition at $B \approx |J_4|/2$ at which the DR order parameter vanishes. For $B \gg |J_4| \gg 1$, the GS has $T^x_i = S^x_i = +1$, which is equivalent to $\sigma^x_{1,i} = \sigma^x_{2,i} = +1$. Thus, this high-field phase must be smoothly connected with the PM phase found in the regime $B \gg 1 \gg |J_4|$. Note that once we restore the interleg coupling $J^z_\perp = 1$, corresponding to the last term in the first line of Eq. (2), the expectation value $L^{-1}\sum_i\langle T^z_i\rangle$ becomes nonzero throughout the entire phase diagram. We stress that the order parameter of the DR phase is the staggered part of $\langle T^z_i\rangle$, whereas the FM phase is characterized by $\langle S^z_i\rangle$, $\langle T^z_i S^z_i\rangle \neq 0$. While the above analysis predicts only DR order for $-J_4 \gg 1$, nothing precludes the coexistence of DR and FM orders at intermediate couplings. In fact, for the classical model with $J_4 < -3/2$, the subspace of degenerate GSs contains states with nonzero total magnetization that satisfy the constraint $T^z_{i+1} = -T^z_i$. In Sec. IV we shall see that DR and FM orders coexist for $J_4 \sim -1.5$ at weak fields.

III. METHODOLOGY

As stated in the Introduction, the purpose of this paper is to determine the GS phase diagram of the model and to characterize the universality classes of the critical lines using the entanglement entropy. Before presenting our results, and for the sake of clarity, let us briefly discuss how to infer the critical behavior from the scaling of the Rényi entanglement entropies near second-order phase transitions.

Consider a one-dimensional system composed of subsystems $\mathcal{A}$ with x sites ($x = 1, \ldots, L$) and $\mathcal{B}$ with $L - x$ sites. The α-Rényi entanglement entropies (REE) of the GS are

defined as

$$S_\alpha(L, x) = \frac{1}{1-\alpha}\ln\mathrm{Tr}\left(\rho^\alpha_\mathcal{A}\right), \qquad (8)$$

where $\rho_\mathcal{A} = \mathrm{Tr}_\mathcal{B}\rho$, constructed from the GS, is the reduced density matrix of the subsystem $\mathcal{A}$. The von Neumann entropy, also known as entanglement entropy, corresponds to $\alpha \to 1$.

The scaling of the REE of the GS is universal and we can explore this universality to determine the critical behavior of the model. For *noncritical* systems, the REE satisfies the entropic area law (see Ref. [49] for a review). For one-dimensional systems, the entropy is expected to approach a constant value at large subsystem sizes, i.e., $S_\alpha(L, x \gg 1) \to b_\alpha$. On the other hand, for *critical* systems with PBC, the REE is expected to behave in the scaling regime $1 \ll x \ll L$ as

$$S^{\mathrm{crit}}_\alpha(L, x) = S^{\mathrm{CFT}}_\alpha(L, x) + S^{\mathrm{USC}}_\alpha(L, x). \qquad (9)$$

The first term on the right-hand side of the above equation is the leading correction predicted by the conformal field theory (CFT) and is given by [50–53]

$$S^{\mathrm{CFT}}_\alpha = \frac{c}{6}\left(1 + \frac{1}{\alpha}\right)\ln\left[\frac{L}{\pi}\sin\left(\frac{\pi x}{L}\right)\right] + a_\alpha, \qquad (10)$$

where c is the central charge and a_α is a nonuniversal constant.

The unusual subleading correction S^{USC}_α has the following universal scaling [54–59]:

$$S^{\mathrm{USC}}_\alpha = g_\alpha \cos(\kappa x + \phi)\left|\sin\left(\frac{\pi x}{L}\right)\right|^{-p_\alpha}, \qquad (11)$$

where g_α is another nonuniversal constant and the exponent p_α is related to the scaling dimension of the energy operator X_ϵ by $p_\alpha = \frac{2X_\epsilon}{\alpha}$. The wave vector κ and the phase ϕ depend on the model. For instance, $\kappa = 0 = \phi$ for the Ising model and $\kappa = \pi, \phi = 0$ for the spin-s XXZ chains at zero magnetic field [58]. For the XXX chain, the scaling is affected by a marginal operator that accounts for logarithmic corrections. As a result, we must replace the central charge in Eq. (10) by [59]

$$c_{\mathrm{eff}} = c + \frac{1}{b^2}\left[\frac{2g}{1 + \pi gb\ln\left[\frac{L}{\pi}\sin\left(\frac{\pi x}{L}\right)\right]}\right]^3, \qquad (12)$$

where g is a constant and b is a universal coefficient in the operator product expansion of the CFT.

It is possible to explore the above scaling laws to determine the critical behavior, as the procedure outlined in Ref. [60], which we use here and explain in the following. For a fixed value of the four-spin interaction, the pseudocritical transverse field B^L_c is given by the maximum value of the entanglement entropy difference (MVEED) defined by

$$\Delta S_1(L, B) = S_1(L, x = L/2) - S_1(L, x = L/4). \qquad (13)$$

Thus, according to the different scalings of critical and noncritical behavior presented above (see Ref. [60] for more details), as $L \to \infty$, we should have

$$\Delta S_1(L, B) = \begin{cases} \frac{c}{6}\ln(2), & B = B^L_c, \\ 0, & B \neq B^L_c. \end{cases} \qquad (14)$$

Note that one can use the above equation to get not only the critical value of B, but also the finite-size estimate of the central charge, given by $c^L = 6\Delta S_1(L, B^L_c)/\ln(2)$. Besides, we

TABLE I. Finite-size estimates of B_c^L and c^L for $J_4 = 0$ obtained from the MVEED method; see Eqs. (13) and (14).

	B_c^L at $J_4 = 0$	
L	B_c^L	c^L
8	1.82660	0.50721
16	1.83171	0.50122
20	1.83194	0.50077
24	1.83213	0.50052
28	1.83214	0.50038
extr.	1.83214(5)	

can also estimate the dimension of the energy operator X_ϵ by fitting the numerical data with the following difference [58]:

$$d_\alpha(L, x) = S_\alpha(L, x) - \frac{c}{6}\left(1 + \frac{1}{\alpha}\right) \ln\left[\frac{L}{\pi}\sin\left(\frac{\pi x}{L}\right)\right], \quad (15)$$

which, asymptotically, behaves as

$$d_\alpha(L, x) = a_\alpha + g_\alpha \cos(\kappa\ell + \phi)\left|\sin\left(\frac{\pi x}{L}\right)\right|^{-p_\alpha}. \quad (16)$$

In order to compute the REE of the GS of the two-leg ladder model described in Sec. II, we have used the standard DMRG approach keeping up to $m = 400$ states per block and the discarded weight was typically 10^{-10}–10^{-12}, in most of the cases. For the multicritical point, where $c = 1$, we kept up to $m = 1000$ states and the discarded weight was typically 10^{-8}–10^{-10}. In this later case we have compared the entanglement entropy with different values of $600 < m < 1000$, and found that it has converged.

IV. RESULTS

We obtain the phase diagram by following the procedure described in Sec. III and computing the desired quantities for different values of system size L. In what follows, we have considered mostly lengths ranging from $L = 8$ to $L = 28$. In some instances, such as when computing the energy exponent or the DR order parameter, we have also used lengths up to $L = 60$.

A. Phase diagram and critical behavior

First, we illustrate how accurate estimates of the critical points $B_c(J_4)$, as well of the central charge c, can be obtained using the procedure discussed above. Here we use PBC. Table I shows a representative example of the finite-size estimates of B_c^L and c^L obtained from the maximum value of $\Delta S_1(L, B)$ for $J_4 = 0$. We clearly see that the transition from the FM to the PM phase at $J_4 = 0$ has central charge $c = 1/2$, and is therefore in the same university class as the critical point of the transverse-field Ising chain.

The finite-size estimates for the critical field for $J_4 = 0$ in Table I are consistent with the value $B_c = 1.838$ found in Ref. [61]. The estimate in Ref. [61] was determined after extrapolating the data for a two-leg ladder with open boundary conditions to the thermodynamic limit $L \to \infty$. A similar extrapolation is performed in Fig. 2, where we show the results
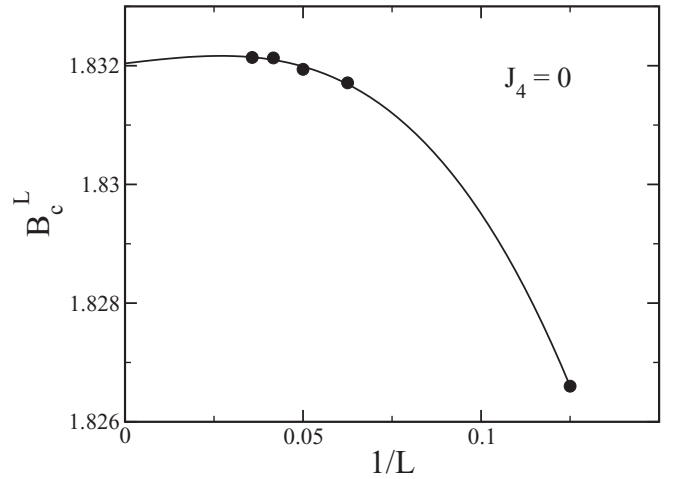

FIG. 2. Critical transverse field B_c^L for $J_4 = 0$, estimated from the maximum value of the entanglement entropy, as a function of $1/L$. The solid line is a fit to Eq. (17).

for the critical field from Table I, as a function of the inverse length, fitted according to the scaling equation

$$B_c^L = B_c + aL^{-1/\nu}(1 + bL^{-\omega}), \quad (17)$$

where B_c is the critical field in the thermodynamic limit, a and b are nonuniversal constants, and $\nu = 1$ and $\omega = 2$ are the correlation length and correction-to-scaling Ising critical exponents, respectively. We obtain the extrapolated value $B_c = 1.83214(5)$, which we believe is more accurate than the previous value from Ref. [61].

We have also determined B_c^L and c^L for several other values of J_4 and system sizes L. Similarly to the results for $J_4 = 0$ in Table I, the critical fields for $L = 28$ are already in excellent agreement with the extrapolation to the thermodynamic limit. For this reason, in Fig. 3 we present the critical lines estimated from data for $L = 28$.

Our numerical results in Fig. 3 reveal the presence of two critical lines, both with central charge $c = 1/2$, which cross at a multicritical point. As discussed in Sec. II, at large $|J_4|$ the critical line corresponds to the Ising transition from the DR to the PM phase. Thus, the dashed line in Fig. 3 can be associated with the spontaneous breaking of lattice translational symmetry. In contrast, the solid line represents the Ising transition at which the spin-rotation $\mathcal{R}$ symmetry is broken. By this reasoning we expect that in the region below the multicritical point both symmetries are broken, leading to a coexistence of the FM and DR phases. We will confirm this picture by computing the order parameters in Sec. IV B. In the following we proceed with characterizing the multicritical point.

The finite-size estimates of c^L indicate that the central charge is larger at the crossing of the two Ising transition lines. We locate the multicritical point (B^{mc}, J_4^{mc}) precisely by finding the maximum value of $\Delta S_L(B, J_4)$ in the J_4-B plane. The same procedure was used in Ref. [60] to determine the tricritical point of the Blume-Capel model. In Table II we present the finite-size estimates of the multicritical couplings obtained by this procedure, together with the estimates of the central charge c^L. We clearly see that the universality class of the multicritical point is described by a CFT with $c = 1$.
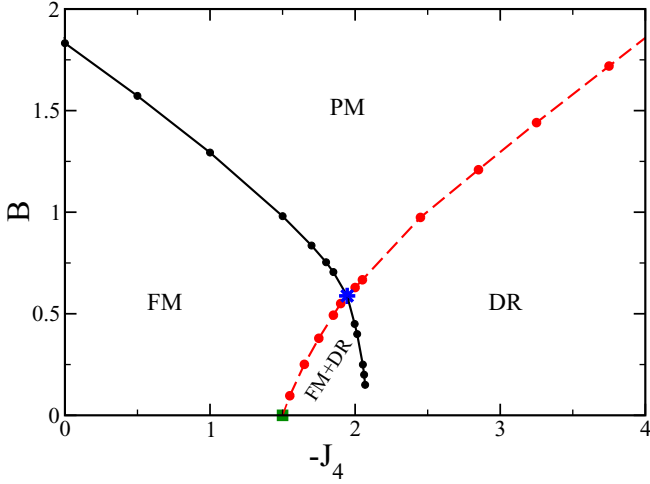
FIG. 3. Phase diagram of the two-leg ladder as a function of the *negative* of the four-spin interaction J_4 and transverse field B, showing the ferromagnetic (FM), dimerized-rung (DR), and paramagnetic (PM) phases. The circles are the numerical finite-size estimates of the critical points for system size $L = 28$. The solid and dashed lines correspond to Ising transitions. The square at $B = 0, J_4 = -3/2$ corresponds to a classical transition point and the star, at the crossing of the critical lines, to a multicritical point. Below the multicritical point there is a region of coexistence of FM and DR order parameters.

Phenomenologically, the central charge can be understood in terms of two independent Majorana fermions which become massless at the Ising transitions represented by the lines in Fig. 3. Since these transitions break different symmetries, there is no direct coupling between the order parameters of these two Ising CFTs. At the multicritical point, the two species of massless Majorana fermions can be combined to define a complex fermion, which can then be bosonized [62]. Thus, this point belong to the Gaussian universality class, and the effective field theory with $c = 1$ can be written in terms of a single massless boson. This theory allows for local operators whose scaling dimension varies continuously as a function of a Luttinger parameter $K = K(B^{\mathrm{mc}}, J_4^{\mathrm{mc}})$. The effective field theory for the multicritical point is discussed in more detail in the Appendix.

To strengthen the case for the crossing of two Ising transitions, we determine the scaling dimension X_ϵ of the energy operator using the fitting procedure summarized by Eqs. (15) and (16). In Fig. 4(a) we present a representative example of the difference $d_2(L, x)$ as a function of x for $J_4 = -1$ and

TABLE II. Finite-size estimates of B^{mc} and J_4^{mc}, and c^L for the multicritical point.

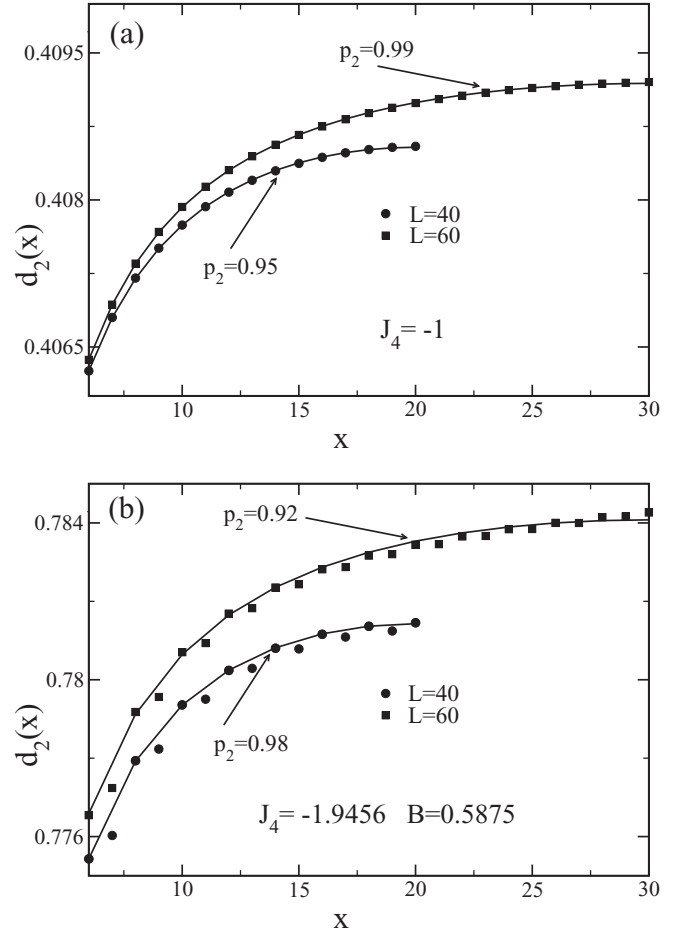| L	J_4^{mc}	B^{mc}	c^L
8	1.9381	0.5925	1.1451
12	1.9395	0.5753	1.0701
16	1.9446	0.5877	1.0504
20	1.9450	0.5863	1.0214
24	1.9452	0.5879	1.0132
28	1.9456	0.5875	1.0109

FIG. 4. Results for $d_2(L, x)$ versus x for the two-leg ladder model with PBC. (a) Data for $J_4 = -1$ and two values of L (see legend). (b) Same as (a), but for the multicritical point. The symbols are the numerical data and the solid lines connect the fitted points using Eq. (16) with $c = 1/2$ in (a) and $c = 1$ in (b). The arrows indicate the values of $p_2 \equiv X_\epsilon$ obtained through the fit. We discarded the first four points of d_2 in the fit procedure.

two system sizes: $L = 40$ and $L = 60$. We performed similar fits along the entire critical lines and obtained the exponent $p_2 = X_\epsilon \approx 1$. These results are consistent with the fact the universality class of critical behavior of these critical lines is the same as the quantum Ising chain, where $c = 1/2$ and $X_\epsilon = 1$.

We also estimate X_ϵ at the multicritical point where $c = 1$. It is important to mention here that, for large system sizes, it is necessary to use more states per block in the DMRG procedure. For this reason, at the multicritical point we use $m = 1000$ states per block. In Fig. 4(b) we show the difference $d_2(L, x)$ at the multicritical point. Note that in this case the subleading corrections exhibit oscillations. Similar oscillations are routinely observed in the Rényi entropy of critical systems described by $c \geqslant 1$ CFTs and presenting tendency of antiferromagnetic order, for instance the spin-1/2 XXZ chain [57]. In that case, the gapless bosonic mode of the $c = 1$ CFT arises naturally from the $U(1)$ symmetry of the model. By contrast, in our model the $U(1)$ symmetry of the low-energy fixed point is emergent and requires fine

tuning to the multicritical point. In our present case, it seems that the origin of the oscillations comes from the dimerization, which also alternate the spins in the lattice in analogy to the antiferromagnetic order. To remove the effect of the oscillations and make the analysis easier, we fit the numerical data using Eq. (16) considering only x even. Our results indicate that $X_\epsilon \approx 1$ at the multicritical point.

B. Order parameters

We close this section by presenting results for the order parameter associated with the DR and FM phases. For practical purposes, instead of using Eq. (6), we consider the parameter defined locally on a four-site plaquette

$$D_i = \tfrac{1}{2}\big|\langle \sigma^z_{1,i+1}\sigma^z_{2,i+1} - \sigma^z_{1,i}\sigma^z_{2,i}\rangle\big|. \qquad (18)$$

Clearly, in the translationally invariant GSs for the FM and PM phases we have $D_i = 0$ for any plaquette. Inside the DR phase, however, we must be careful because $D_i = 0$ for any *finite* system with PBC. In order to investigate the symmetry breaking by considering finite systems, we add a small perturbation that selects one of the two DR GSs which become exactly degenerate in the thermodynamic limit. A simple way to lift this degeneracy is to consider a system with semi-open boundary conditions (SOBC), consisting of an open ladder with L odd to which we add the following term that connects the two edges:

$$H^{DR}_{BC} = -\big(\sigma^z_{1,1}\sigma^z_{1,L} + \sigma^z_{2,1}\sigma^z_{2,L}\big). \qquad (19)$$

Similarly, we can view this SOBC as the ladder with PBC in which we suppress the four-spin interaction of the Lth plaquette. We then consider the order parameter at the center of the ladder, $D_{(L+1)/2}$, far from the perturbation at the boundary.

To illustrate the behavior of the DR order parameter, we first present in Fig. 5(a) the result for $D_{(L+1)/2}$ as a function of J_4 for $B = 1$ and different values of system size L. Note that, according to the phase diagram in Fig. 3, as we vary J_4 at fixed $B = 1$, we cut across three different phases. As expected, $D_{(L+1)/2}$ is nonzero only in the DR phase. The finite size scaling analysis in Fig. 5(b) confirms that $D_{(L+1)/2}$ approaches a finite value at large values $|J_4|$, providing unambiguous evidence of the DR GS.

We can also locate the transition corresponding to the dashed line in Fig. 3 by analyzing the DR order parameter. For a fixed value of B, we can estimate the critical point J^c_4 as the inflection point of $D_{(L+1)/2}$ as a function of J_4. We find that the estimates of the critical points obtained within this procedure (not shown) are in good agreement with the results from the MVEED.

Finally, we investigate the FM order parameter defined as $M_{(L+1)/2} = \langle \sigma^z_{1,(L+1)/2}\rangle$. Similarly to the DR order parameter, $M_{(L+1)/2}$ vanishes identically for any finite system with PBC. We must then add a local perturbation that breaks the $\mathbb{Z}_2$ spin-rotation symmetry. We consider a weak boundary longitudinal field that scales with system size:

$$H^{FM}_{BC} = -\frac{1}{L^2}\big(\sigma^z_{1,1} + \sigma^z_{2,1}\big). \qquad (20)$$
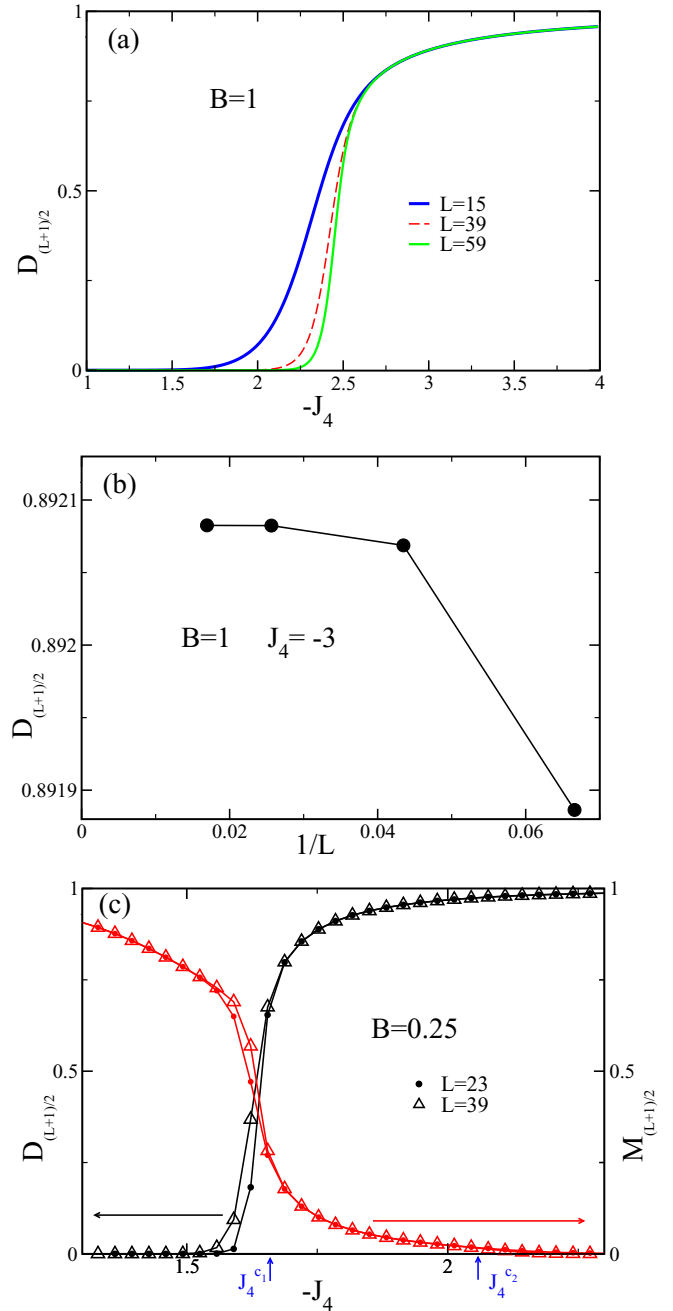

FIG. 5. Order parameters for the phases of the two-leg ladder with a particular boundary condition, see Eq. (19). (a) DR order parameter as a function of J_4 for $B = 1$ and different system sizes L. (b) Finite size scaling of the DR order parameter for $J_4 = -3$ and $B = 1$. (c) $D_{(L+1)/2}$ and $M_{(L+1)/2}$ versus J_4 for $B = 0.25$ and two values of L. The blue arrows in the horizontal axis indicate the positions of the two critical points for $B = 0.25$ according to the phase diagram in Fig. 3. The lines in (b) and (c) connect the numerical data.

In Fig. 5(c) we show the results for $D_{(L+1)/2}$ and $M_{(L+1)/2}$ as a function of J_4 for $B = 0.25$ and two different system sizes. For this value of B we have two critical points, $J^{c_1}_4 \approx -1.65$ and $J^{c_2}_4 \approx -2.05$, which are indicated by blue arrows in the horizontal axis of Fig. 5(c). As we observe in this figure, both

order parameters are nonzero between the two critical points, demonstrating that the FM and DR orders coexist in this range. Finite size effects are more pronounced for $J_4 \approx J_4^{c_1}$. We have performed a finite size scaling analysis similar to the one in Fig. 5(b) and verified that $\lim_{L\to\infty} M_{(L+1)/2}$ is nonzero for some values of J_4 above $J_4^{c_1}$ and below $J_4^{c_2}$.

For $B \ll 1$, the onset of DR order matches the classical transition point $J_4 = -3/2$, see Fig. 3. As discussed in Sec. II, the classical model with $B = 0$ has an exponentially degenerate GS manifold which includes DR states with finite magnetization. Our observation of a coexistence phase implies that, slightly above the classical transition point, an arbitrarily small transverse field lifts the exponential degeneracy and selects four GSs that break both spin-rotation and translational symmetries. These four GSs can be labeled by the signs of $D_{(L+1)/2}$ and $M_{(L+1)/2}$ in the limit $L \to \infty$. In addition, for $B > 0$ there appears the second critical point, beyond which the FM order parameter vanishes and the spin-rotation symmetry is restored, while the translational symmetry remains broken. Using the MVEED, we have not been able to track the transition from the coexistence phase to the DR phase all the way down to $B \to 0$; see the black line in Fig. 3. The numerical difficulties for small B and $-J_4 > 3/2$ are most likely associated with the approximate degeneracy of exponentially many states in this regime. Note from Fig. 5 that the black critical line is smooth around $0.1 < B < 0.5$. This suggests that this line will touch the horizontal axis at $-J_4^c \approx 2$. However, when treating the classical system ($B = 0$), we find a single transition at $J_4^c = -3/2$ from the ferromagnetic phase to the regime of highly degenerate ground states, containing DR states with or without ferromagnetic order. Due to this fact, a reentrance of the pure DR phase cannot be ruled out, and our data are inconclusive for $B < 0.1$.

V. CONCLUSIONS

We investigated a transverse-field two-leg Ising ladder with a plaquette four-spin interaction. We obtained the ground state phase diagram by exploring the finite-size scaling entanglement entropy. We found two critical lines that separate two ordered phases (see Fig. 3): a ferromagnetic and a dimerized-rung phase. These phases spontaneously break the symmetries of $\mathbb{Z}_2$ spin rotation and translation by one site, respectively. The universality class of both transitions is the same as the quantum Ising chain. We confirmed this critical behavior by calculating the central charge using the entanglement entropy. We found that the critical lines with central charge $c = 1/2$ cross at a multicritical point with $c = 1$ (see Table II). By analyzing the subleading corrections of the scaling Rényi entanglement entropy, we were able to determine the scaling dimension X_ϵ of the energy operator. Our results support $X_\epsilon = 1$ along the critical lines, as expected for models with $c = 1/2$, as well as at the multicritical point. By investigating the order parameters, we found a region in parameter space where the ferromagnetic and dimerized-rung orders coexist (see Fig. 5). It is interesting to notice that the plaquette symmetry of the four-spin interaction seems to be responsible for the richness of the phase diagram presented by this model. In contrast, the transverse-field chain in the regime of dominant linear four-spin interaction has only an eightfold ground state degeneracy

and a first-order transition to the disordered state takes place instead, with the multicritical point located at zero transverse field [10].

APPENDIX: EFFECTIVE FIELD THEORY FOR THE MULTICRITICAL POINT

In this Appendix we analyze the effective field theory that describes the vicinity of the multicritical point with $c = 1$ in the two-leg ladder model. Since the multicritical point appears at intermediate couplings, far from any exactly solvable point in the phase diagram, we adopt a phenomenological approach guided by symmetry considerations. We can cast the order parameters of the model in terms of two $\mathbb{Z}_2$ symmetries: the spin-rotation symmetry $\mathcal{R}$ and the symmetry of exchanging even and odd sublattices upon translation by one site. Let $\sigma_1(x)$ and $\sigma_2(x)$ denote the order operators in the Ising CFTs [63] that describe the low-energy physics near the transitions where these $\mathbb{Z}_2$ symmetries are spontaneously broken. The order operators have conformal weights $(\frac{1}{16}, \frac{1}{16})$. The FM phase corresponds to $\langle\sigma_1\rangle \neq 0$, $\langle\sigma_2\rangle = 0$, whereas the DR phase corresponds to $\langle\sigma_1\rangle = 0$, $\langle\sigma_2\rangle \neq 0$. In the coexistence phase we have $\langle\sigma_1\rangle \neq 0$ and $\langle\sigma_2\rangle \neq 0$.

The effective Hamiltonian density for the perturbed CFT including all local operators allowed by symmetry is

$$\mathcal{H}_{\text{eff}} = \sum_{n=1,2} \left[\frac{iv_n}{2}(\xi_n\partial_x\xi_n - \bar{\xi}_n\partial_x\bar{\xi}_n) + im_n\xi_n\bar{\xi}_n \right] + g\xi_1\bar{\xi}_1\xi_2\bar{\xi}_2,$$

where $\xi_n(x)$ and $\bar{\xi}_n(x)$ are chiral Majorana fermions with conformal weights $(\frac{1}{2}, 0)$ and $(0, \frac{1}{2})$, respectively, which obey $\{\xi_n(x), \xi_{n'}(x')\} = \{\bar{\xi}_n(x), \bar{\xi}_{n'}(x')\} = \delta_{nn'}\delta(x - x')$ and $\{\xi_n(x), \bar{\xi}_{n'}(x')\} = 0$. The operators $\epsilon_n = i\xi_n\bar{\xi}_n$, with conformal weights $(\frac{1}{2}, \frac{1}{2})$ and scaling dimension $X_\epsilon = 1$, can be identified with the energy operators in the Ising CFTs. The velocities v_1 and v_2 can be different since the two species of Majorana fermions are not related by symmetry. The masses m_1 and m_2 can also be different and represent the couplings constants for the leading relevant operators in the effective Hamiltonian. Importantly, the term $\sigma_1\sigma_2$, which would be a strongly relevant perturbation, is not allowed because the order parameters change sign under different $\mathbb{Z}_2$ symmetries.

As a result, the leading interaction between the two Ising models is the quartic interaction with coupling constant g.

The CFT with a single gapless Majorana fermion has central charge $c = 1/2$. Thus, the critical lines in the phase diagram in Fig. 3 are defined by the condition that one of the masses goes through zero while the other one remains finite. At the crossing of these lines, we have $m_1 = m_2 = 0$. At this point the CFT of two decoupled Ising models is only perturbed by the quartic interaction with coupling constant g. To analyze the effects of this interaction, we define a complex fermion from the linear combination of the Majorana fermions:

$$\psi = \frac{\xi_1 + i\xi_2}{\sqrt{2}}, \quad \bar{\psi} = \frac{\bar{\xi}_1 + i\bar{\xi}_2}{\sqrt{2}}.$$

We can then bosonize the chiral complex fermions in the form $\psi \sim e^{-i\sqrt{\pi}(\theta+\phi)}$, $\bar{\psi} \sim e^{-i\sqrt{\pi}(\theta-\phi)}$, where $\phi(x)$ and $\theta(x)$ are dual bosonic fields that obey $[\phi(x), \partial_{x'}\theta(x')] = i\delta(x - x')$ [62]. The bosonized Hamiltonian density for $m_1 = m_2 = 0$

has the form

$$\mathcal{H}_{\text{eff}}^{\text{mc}} = \frac{vK}{2}(\partial_x\theta)^2 + \frac{v}{2K}(\partial_x\phi)^2 + \lambda_1\cos(4\sqrt{\pi}\phi)$$
$$+ \lambda_2\cos(4\sqrt{\pi}\theta) + \lambda_3\cos(\sqrt{4\pi}\theta)\cos(\sqrt{4\pi}\phi),$$

where v is the renormalized velocity, K is the Luttinger parameter, and the cosine terms have coupling constants $\lambda_1, \lambda_2 \sim g$ and $\lambda_3 \sim v_1 - v_2$. For $g = 0$ we have $K = 1$, corresponding to free fermions. The λ_3 term, associated with the velocity mismatch, has scaling dimension $K + K^{-1}$ and is irrelevant for any $K \neq 1$. The λ_1 and λ_2 terms have scaling dimensions $4K$ and $4/K$, respectively. As a result, they are both irrelevant for a wide range of the Luttinger parameter, $1/2 < K < 2$. Dropping the irrelevant operators, we conclude that the low-energy fixed point at the crossing of the critical lines corresponds to a free boson, with central charge $c = 1$. The scaling dimensions of local operators depend on the value of the Luttinger parameter, which is not fixed by any symmetries.

[1] J. B. Parkinson and D. J. J. Farnell, *An Introduction to Quantum Spin Systems*, Lecture Notes in Physics, Vol. 816 (Springer, Berlin, 2010).

[2] W. D. Ratcliff and W. Lynn, *Neutron Scattering - Magnetic and Quantum Phenomena, Experimental Methods in the Physical Sciences*, edited by F. Fernandez-Alonso and D. L. Price (Elsevier, Cambridge, 2015), Vol. 48.

[3] P. A. Lee, N. Nagaosa, and X.-G. Wen, Rev. Mod. Phys. **78**, 17 (2006).

[4] J. Cho, Y. Fujii, K. Konioshi, J. Yoon, N. Kim, J. Jung, S. Miwa, M. Jung, Y. Suzuki, and C. You, J. Magn. Magn. Mater. **409**, 99 (2004).

[5] I. Žutić, F. Jaroslav, and S. Das Sarma, Rev. Mod. Phys. **76**, 323 (2004).

[6] J. L. Jimenez, S. P. G. Crone, E. Fogh *et al.*, Nature (London) **592**, 370 (2021).

[7] P. R. C. Guimarães, J. A. Plascak, O. F. de Alcantara Bonfim, and J. Florencio, Phys. Rev. E **92**, 042115 (2015).

[8] B. Boechat, J. Florencio, A. Saguia, and O. F. de Alcantara Bonfim, Phys. Rev. E **89**, 032143 (2014).

[9] O. F. de Alcantara Bonfim, A. Saguia, B. Boechat, and J. Florencio, Phys. Rev. E **90**, 032101 (2014).

[10] O. F. de Alcantara Bonfim and J. Florencio, Phys. Rev. B **74**, 134413 (2006).

[11] G. T. Hohensee, R. B. Wilson, J. P. Feser, and D. G. Cahill, Phys. Rev. B **89**, 024422 (2014).

[12] M. S. Naseri and S. Mahdavifar, Physica A **474**, 107 (2017).

[13] A. Jabar, N. Tahiri, K. Jetto, and L. Bahmad, Superlattices Microstruct. **104**, 46 (2017).

[14] W. Chunle, Q. Zikai, and Z. Jinghbo, Ferroelectrics **77**, 21 (1988).

[15] B. H. Teng and H. K. Sy, Europhys. Lett. **73**, 601 (2006).

[16] P. Kowalewska and K. Szalowski, J. Magn. Magn. Mater. **496**, 165933 (2020).

[17] J. Torrico and J. A. Plascak, Phys. Rev. E **102**, 062116 (2020).

[18] K. Szalowski and P. Kowalewska, Materials **13**, 485 (2020).

[19] S. Thomas, S. Ramasesha, K. Hallberg, and D. Garcia, Phys. Rev. B **86**, 180403(R) (2012).

[20] A. Valentim, G. A. Bocan, J. D. Fuhr, D. J. Garcia, G. Giri, M. Kumar, and S. Ramasesha, Phys. Chem. Chem. Phys. **22**, 5882 (2020).

[21] C. Karrasch, D. M. Kennes, and F. Heidrich-Meisner, Phys. Rev. B **91**, 115130 (2015).

[22] Z. Liu, S. Jiang, X. Kong, and Y. Xu, Physica A **473**, 536 (2017).

[23] A. H. MacDonald, S. M. Girvin, and D. Yoshioka, Phys. Rev. B **37**, 9753 (1988).

[24] O. I. Motrunich, Phys. Rev. B **72**, 045105 (2005).

[25] S. Brehmer, H.-J. Mikeska, M. Müller, N. Nagaosa, and S. Uchida, Phys. Rev. B **60**, 329 (1999).

[26] M. Matsuda, K. Katsumata, R. S. Eccleston, S. Brehmer, and H.-J. Mikeska, Phys. Rev. B **62**, 8903 (2000).

[27] R. Coldea, S. M. Hayden, G. Aeppli, T. G. Perring, C. D. Frost, T. E. Mason, S.-W. Cheong, and Z. Fisk, Phys. Rev. Lett. **86**, 5377 (2001).

[28] C. B. Larsen, A. T. Romer, S. Janas, F. Treue, B. Monsted, N. E. Shaik, H. M. Ronnow, and K. Lefmann, Phys. Rev. B **99**, 054432 (2019).

[29] T. Cookmeyer, J. Motruk, and J. E. Moore, Phys. Rev. Lett. **127**, 087201 (2021).

[30] G. Chaboussant, P. A. Crowell, L. P. Lévy, O. Piovesana, A. Madouri, and D. Mailly, Phys. Rev. B **55**, 3046 (1997).

[31] B. C. Watson, V. N. Kotov, M. W. Meisel, D. W. Hall, G. E. Granroth, W. T. Montfrooij, S. E. Nagler, D. A. Jensen, R. Backov, M. A. Petruska, G. E. Fanucci, and D. R. Talham, Phys. Rev. Lett. **86**, 5168 (2001).

[32] T. Hong, Y. H. Kim, C. Hotta, Y. Takano, G. Tremelling, M. M. Turnbull, C. P. Landee, H.-J. Kang, N. B. Christensen, K. Lefmann, K. P. Schmidt, G. S. Uhrig, and C. Broholm, Phys. Rev. Lett. **105**, 137207 (2010).

[33] D. Schmidiger, P. Bouillot, T. Guidi, R. Bewley, C. Kollath, T. Giamarchi, and A. Zheludev, Phys. Rev. Lett. **111**, 107202 (2013).

[34] D. Blosser, V. K. Bhartiya, D. J. Voneshen, and A. Zheludev, Phys. Rev. Lett. **121**, 247201 (2018).

[35] D. C. Cabra, A. Honecker, and P. Pujol, Phys. Rev. Lett. **79**, 5126 (1997).

[36] A. Honecker, F. Mila, and M. Troyer, Eur. Phys. J. B. **15**, 227 (2000).

[37] J.-B. Fouet, F. Mila, D. Clarke, H. Youk, O. Tchernyshyov, P. Fendley, and R. M. Noack, Phys. Rev. B **73**, 214405 (2006).

[38] O. A. Starykh and L. Balents, Phys. Rev. Lett. **93**, 127202 (2004).

[39] T. Hikihara and O. A. Starykh, Phys. Rev. B **81**, 064432 (2010).

[40] G. Barcza, O. Legeza, R. M. Noack, and J. Sólyom, Phys. Rev. B **86**, 075133 (2012).

[41] T. Sakai and Y. Hasegawa, Phys. Rev. B **60**, 48 (1999).

[42] A. Läuchli, G. Schmid, and M. Troyer, Phys. Rev. B **67**, 100409(R) (2003).

[43] C. J. Calzado, C. de Graaf, E. Bordas, R. Caballol, and J.-P. Malrieu, Phys. Rev. B **67**, 132409 (2003).

[44] V. Gritsev, B. Normand, and D. Baeriswyl, Phys. Rev. B **69**, 094431 (2004).

[45] G.-H. Liu, H.-L. Wang, and G.-S. Tian, Phys. Rev. B **77**, 214418 (2008).

[46] S. Capponi, P. Lecheminant, and M. Moliner, Phys. Rev. B **88**, 075132 (2013).

[47] M. Kohmoto, M. den Nijs, and L. P. Kadanoff, Phys. Rev. B **24**, 5229 (1981).

[48] F. C. Alcaraz, M. N. Barber, and M. T. Batchelor, Phys. Rev. Lett. **58**, 771 (1987).

[49] J. Eisert, M. Cramer, and M. B. Plenio, Rev. Mod. Phys. **82**, 277 (2010).

[50] C. Holzhey, F. Larsen, and F. Wilczek, Nucl. Phys. B **424**, 443 (1994).

[51] P. Calabrese and J. Cardy, J. Stat. Mech. (2004) P06002.

[52] P. Calabrese and J. Cardy, J. Phys. A: Math. Theor. **42**, 504005 (2009).

[53] I. Affleck and A. W. W. Ludwig, Phys. Rev. Lett. **67**, 161 (1991).

[54] P. Calabrese, M. Campostrini, F. Essler, and B. Nienhuis, Phys. Rev. Lett. **104**, 095701 (2010).

[55] P. Calabrese and F. H. L. Essler, J. Stat. Mech. (2010) P08029.

[56] M. Fagotti and P. Calabrese, J. Stat. Mech. (2011) P01017.

[57] J. C. Xavier and F. C. Alcaraz, Phys. Rev. B **83**, 214425 (2011).

[58] J. C. Xavier and F. C. Alcaraz, Phys. Rev. B **85**, 024418 (2012).

[59] J. Cardy and P. Calabrese, J. Stat. Mech. (2010) P04023.

[60] J. C. Xavier and F. C. Alcaraz, Phys. Rev. B **84**, 094410 (2011).

[61] J. C. Xavier and F. B. Ramos, J. Stat. Mech. (2014) P10034.

[62] A. O. Gogolin, A. A. Nersesyan, and A. M. Tsvelik, *Bosonization and Strongly Correlated System* (Cambridge University Press, Cambridge, 1998).

[63] P. Di Francesco, P. Mathieu, and D. Senechal, *Conformal Field Theory* (Springer, New York, 1999).